Application of a fluorescent cobalamin analogue for analysis of the binding kinetics

A study employing recombinant human transcobalamin and intrinsic factor

Sergey N. Fedosov[1], Charles B. Grissom[2], Natalya U. Fedosova[3], Søren K. Moestrup[4], Ebba Nexø[5] and Torben E. Petersen[1]

1 Protein Chemistry Laboratory, Department of Molecular Biology, University of Aarhus, Denmark
2 Department of Chemistry, University of Utah, Salt Lake City, UT, USA
3 Department of Physiology and Biophysics, University of Aarhus, Denmark
4 Department of Medical Biochemistry, University of Aarhus, Denmark
5 Department of Clinical Biochemistry, AS Aarhus University Hospital, Denmark

Fluorescent probe rhodamine was appended to 5′ OH-ribose of cobalamin (Cbl). The prepared conjugate, CBC, bound to the transporting proteins, intrinsic factor (IF) and transcobalamin (TC), responsible for the uptake of Cbl in an organism. Pronounced increase in fluorescence upon CBC attachment facilitated detailed kinetic analysis of Cbl binding. We found that TC had the same affinity for CBC and Cbl ($K_d = 5 \times 10^{-15}$ M), whereas interaction of CBC with the highly specific protein IF was more complex. For instance, CBC behaved normally in the partial reactions CBC + IF_{30} and CBC + IF_{20} when binding to the isolated IF fragments (domains). The ligand could also assemble them into a stable complex IF_{30}–CBC–IF_{20} with higher fluorescent signal. However, dissociation of IF_{30}–CBC–IF_{20} and IF–CBC was accelerated by factors of 3 and 20, respectively, when compared to the corresponding Cbl complexes. We suggest that the correct domain–domain interactions are the most important factor during recognition and fixation of the ligands by IF. Dissociation of IF–CBC was biphasic, and existence of multiple protein–analogue complexes with normal and partially corrupted structure may explain this behaviour. The most stable component had $K_d = 1.5 \times 10^{-13}$ M, which guarantees the binding of CBC to IF under physiological conditions. The specific intestinal receptor cubilin bound both IF–CBC and IF–Cbl with equal affinity. In conclusion, the fluorescent analogue CBC can be used as a reporting agent in the kinetic studies, moreover, it seems to be applicable for imaging purposes *in vivo*.

Cobalamin (Cbl, vitamin B_{12}) is a cofactor for two crucial enzymes in mammals [1]. Therefore, an enhanced influx of the vitamin is required during cell growth to satisfy high synthetic and energetic demands. Intensive uptake of Cbl was suggested to be a good marker of the fast growing tissues including malignant cells [2]. However, declining application of radioactive ^{57}Co-labeled Cbl prompts investigation of alternative ligands. Imaging of tumours with the help of Cbl derivatives, as well as targeted delivery of

conjugated drugs, is rapidly becoming a perspective direction of Cbl-related research [3,4]. Yet, there is a gap between the number of new derivatives and the detailed knowledge about their interaction with the specific protein carriers, which are the key players in targeted delivery.

Uptake of dietary Cbl is a complex process because only a limited amount of the vitamin is available from natural sources. Three specific proteins, intrinsic factor (IF), transcobalamin (TC) and haptocorrin (HC), are involved in transportation (reviewed in [5–8]). IF is responsible for gastrointestinal uptake of vitamin B_{12}, and this protein is particularly sensitive to any changes introduced into the structure of the ligand. Afterwards, Cbl is transferred to TC, which delivers the vitamin to different tissues via the blood circulation. TC is also quite specific for the 'true' cobalamins. The third carrier HC is present in many body fluids and has low substrate specificity. It is assumed to be a storage, protective or scavenging protein. HC eventually binds all Cbl-resembling molecules and transports them to the liver, where they are either stored or disposed. Yet, the exact function of HC remains unknown.

Affinity of the transporting proteins for Cbl still remains a controversial issue with an extraordinary dispersion of the reported equilibrium dissociation constants $K_d = 10^{-9}-10^{-15}$ M [5,7,10–15]. However, the major reasons of this discrepancy are rather artificial. Thus, insufficient equilibration of two binding species at the point of equivalence, e.g., $E + S \Leftrightarrow ES$ at $E_0 \approx S_0$, leads to severe overestimation of K_d as discussed previously [10]. Inapplicability of the equilibrium methods for a near-irreversible binding was also pointed out by other authors [12]. It was concluded that the separate kinetic determination of k_+ and k_- gives a much more adequate estimation of K_d. Attempts to follow the association and dissociation kinetics were made using radioactive ^{57}Co-labeled Cbl by the charcoal method [5,7,12,13], change in absorbance of Cbl [10,14], and plasmon resonance signal [15]. However, all the above methods were not completely adequate for the task, because partial protein precipitation in the first protocol or low signal to noise ratio in the two latter procedures could compromise the accuracy of measurements. In this respect, application of a highly sensitive fluorescent probe seems to be advantageous in terms of the protein concentrations, time scale and amplitude of response.

Molecular mechanisms of Cbl recognition by the transporting proteins are not completely understood. A probable structural basis of the IF–ligand interactions was recently inferred from the properties of its two pro-

teolytic fragments [9,10]. Thus, the small C-terminal fragment IF_{20} (13 kDa peptide with ≈ 7 kDa of carbohydrates) had a relatively high affinity for Cbl and was suggested to be the primary subject of substrate binding. The larger N-terminal fragment IF_{30} (30 kDa peptide) bound the ligand with low affinity. However, interaction between IF_{30} and the saturated IF_{20}–Cbl complex was necessary to stabilize the bound ligand within a firm sandwich-like complex IF_{30}–Cbl–IF_{20}. In addition, only two assembled fragments could bind to the specific receptor cubilin [10]. Based on these facts, the sequential interaction of Cbl with the two domains of the full length IF was suggested.

The structure of the kindred protein TC (human and bovine) in complex with H_2OCbl was recently solved on the atomic level [16]. The found architecture of the TC–ligand complex was very similar to the one suggested for IF [9,10]. TC consists of two domains with Cbl placed in-between. The ligand was essentially enwrapped, and its solvent accessible surface decreased to $\approx 7\%$ with only the ribose moiety exposed. In total, 34 hydrogen and hydrophobic contacts between TC and the ligand ensured a very strong retention of Cbl. Additionally, a His residue substituted for water of H_2OCbl, which added to protection of the ligand against reduction and coordination of other compounds. The structure of TC–Cbl complex directly indicated that a foreign label (e.g., a fluorescent probe) should be conjugated to 5′ OH ribosyl group of Cbl to minimize loss of affinity.

The present work describes the binding of a fluorescent Cbl analogue CBC-244 to the Cbl-transporting proteins IF and TC. In the interpretation of our results we emphasize the following issues: (i) kinetic characterization of the new ligand; (ii) its applicability in the binding studies of other corrinoids; and (iii) potential pertinence to the physiological studies.

Results

Preparation of the proteins

The experiments were performed on the recombinant human proteins IF and TC purified from plants [17] and yeast [18], respectively. Both proteins were originally obtained as Cbl-saturated holo-forms, and preparation of the unsaturated apo-forms required their denaturing. Unfolding of TC with 5 M guanidine hydrochloride (GdnHCl) was earlier found to be the best in terms of the protein recovery [14,18]. However, similar approach to IF gave some variation in its Cbl binding properties, as discussed elsewhere [10]. In the present study, we have found that denaturing in 8 M

urea followed by a renaturing dilution (see below) provided better recovery of IF and improved its ligand binding properties, as will be demonstrated below.

Synthesis of the fluorescent Cbl analogue CBC-244

The fluorescent conjugate of Cbl (Fig. 1A) was prepared by coupling of 5- (and 6-) carboxyrhodamine succinimidil ester (5/6 mixed isomers) to an amino derivative of Cbl modified at 5′OH-ribose [19,20]; see below for details. Two isomers of CBC-244 were then separated by reverse phase HPLC and examined for their binding to IF and TC. Both derivatives behaved in most respects quite similarly (data not shown), yet, the binding of 5′ CBC-244 to the tested proteins was 1.5-fold faster. The experiments described in the present article were performed with 5′ form, and below we will refer to 5′ CBC-244 as CBC.

Spectral properties of CBC

The coefficient of molar absorbance for rhodamine moiety of CBC was estimated as $\varepsilon_{527} = 90\,000$ M^{-1}·cm^{-1}. In the below experiments we used concentrations of

CBC ≤ 1 μM, where no self-quenching was observed, and the intensity of CBC fluorescence linearly depended on CBC concentration (data not shown). The excitation and emission spectra of CBC, either free or bound to the Cbl-specific proteins, are presented in Fig. 1B. Attachment to the transporting proteins, especially to IF, clearly induced increase in the quantum yield of the fluorescent ligand, allowing direct monitoring of the binding-dissociation reactions. Presence of 2 μM Cbl (cyano-, aquo-, adenosyl-forms) in the solutions together with CBC (both free and protein bound) caused approximately 6% quenching of the fluorescent signal immediately after mixing as demonstrated in Fig. 1C. This effect was insignificant at the Cbl concentrations below 1 μM, but required correction when concentrations increased to 2 μM and above.

Binding of CBC to IF or TC

As a pilot experiment, an isotope dilution assay was conducted, where increasing concentrations of the 'cold' ligand (Cbl or CBC) competed with the radioactive ligand [57]Co-labeled Cbl for the binding to IF (or TC). It appeared that both the analogue and Cbl efficiently displaced [57]Co-labeled Cbl according to the ratio of their half-saturation points $Cbl_{0.5}/CBC_{0.5} =$
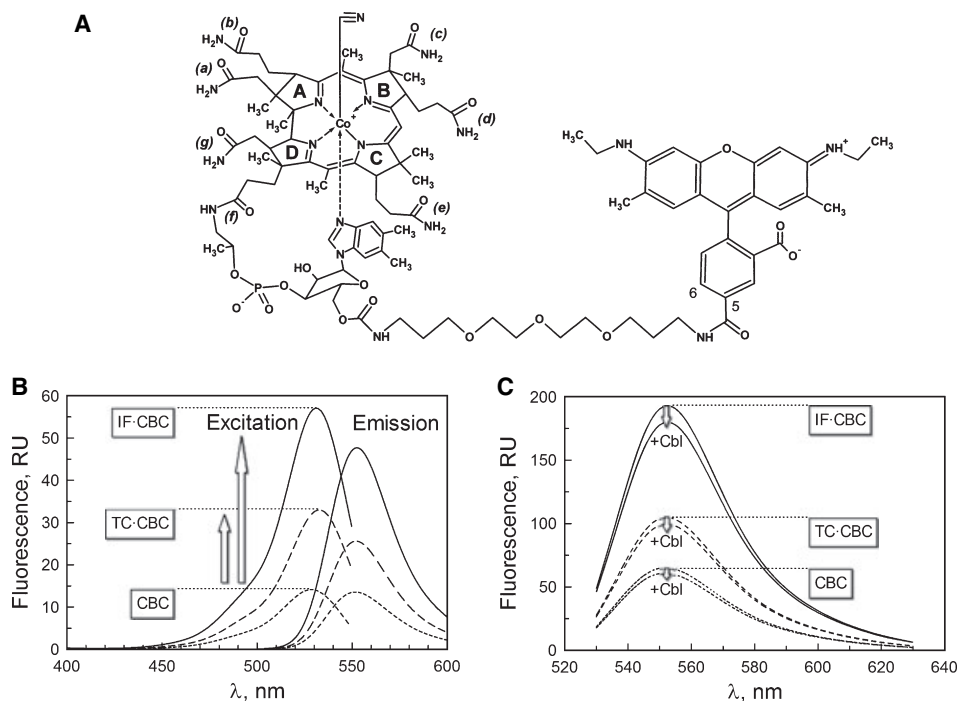

Fig. 1. Fluorescent conjugate 5′ CBC-244. (A) Chemical structural of CBC ($M_r = 2042$). (B) Excitation and emission spectra of CBC in solution or bound to the Cbl specific proteins, [CBC] = 0.5 μM, [TC] = 1 μM, [IF] = 1 μM, pH 7.5, 20 °C. (C) Fluorescence quenching ($F_q = 0.94 \cdot F_0$) induced by 2 μM Cbl in the solution of 0.5 μM CBC (free or bound to TC or IF), incubation time 0.5–1 min.
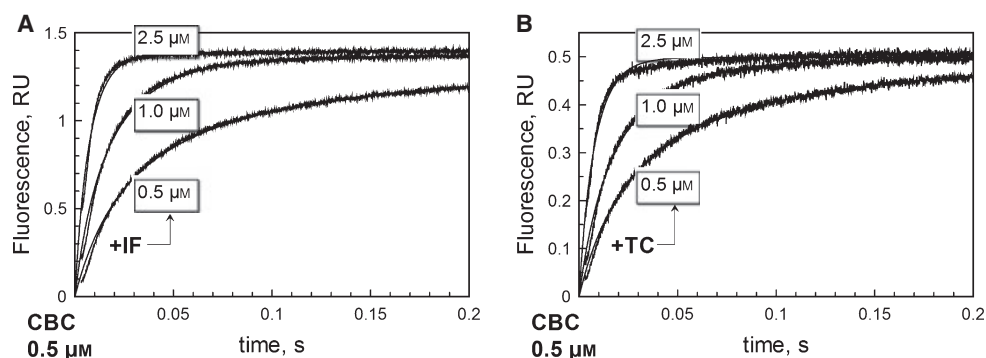
Fig. 2. Binding of CBC to IF and TC. (A) CBC + IF → IF–CBC. (B) CBC + TC → TC–CBC. Both reactions were followed in 0.2 M P_i buffer, pH 7.5, 20 °C. Final concentrations in the cuvette: [CBC] = 0.5 μM, [protein] = 0.5, 1.0, 2.5 μM. See text and Table 1.

0.2 and 0.4 for IF and TC, respectively. Therefore, the fluorescent probe was subjected to further kinetic analysis.

Interaction of CBC with the specific binders was monitored over time, where increasing amplitude of the fluorescent signal reflected binding process (Fig. 2). The experiments were performed with varying protein concentrations keeping the initial concentration of CBC constant. The same final amplitude of fluorescent response was reached after 30 s of incubation, therefore the reactions obeyed an irreversible bimolecular mechanism E + S → ES in the time scale of the experiment. The data were fitted by the corresponding

equation [10]. Both IF and TC demonstrated the same rate constant of CBC binding $k_{+CBC} = 64 \pm 5$ μM^{-1}·s^{-1}. The amplitude of relative response for IF was, however, three-fold higher (Table 1).

Binding of CBC to IF fragments IF$_{20}$ or IF$_{30}$

The binding reactions were conducted at constant CBC and variable concentrations of the peptides IF$_{20}$ and IF$_{30}$ (Fig. 3). The preliminary equilibrium analysis in Fig. 3A indicated that the ligand–peptide interaction was reversible for IF$_{20}$ + CBC and IF$_{30}$ + CBC, but nearly irreversible for the three component mixture

Table 1. Interactions between IF, TC and the ligands CBC, cyano-cobalamin (CNCbl). All reactions were carried out at 20 °C and pH 7.5. The results are presented as mean ± SD. Bold type indicates the rate constant for CBC differing from the corresponding coefficients for Cbl. *Data for H_2OCbl and ^{57}Co-labeled CNCbl from references [9,10,14,18]. RU, response units.

Reaction	ΔFluor. (RU·μM^{-1})	$k_+ \times 10^{-6}$ (M^{-1}·s^{-1})	k_- (s^{-1})	K_d (M)
IF$_{20}$ + L ⇔ IF$_{20}$–L				
L = CBC	0.75 ± 0.05	61 ± 8	9 ± 2	1.5 ± 0.3 × 10^{-7}
L = Cbl	–	≈ 60	≈ 9	≈ 1.5 × 10^{-7}
L = Cbl*	–	14 ± 3	4 ± 3	3 ± 2 × 10^{-7}
IF$_{30}$ + L ⇔ IF$_{30}$–L				
L = CBC	0.82 ± 0.08	2 ± 1	160 ± 30	**8 ± 4** × 10^{-5}
L = Cbl*	–	3.5 ± 0.6	140 ± 40	4.0 ± 2 × 10^{-5}
IF$_{20}$–L + IF$_{30}$ ⇔ IF$_{20}$–L–IF$_{30}$				
L = CBC	2.0 ± 0.1	4.2 ± 0.4	**1.2 ± 0.3 × 10^{-3}**	**2.9 ± 0.7 × 10^{-10}**
L = Cbl	–	≈ 4	5.0 ± 1.5 × 10^{-4}	≈ 10^{-10}
L = Cbl*	–	4.0 ± 0.5	≈ 10^{-4}	≈ 10^{-11}
IF + L ⇔ IF–L				
L = CBC	2.7 ± 0.1	64 ± 6	**(65%) 8 × 10^{-6}**	**1.2 ± 0.2 × 10^{-13}**
			(25%) 2 × 10^{-4}	**3.1 ± 0.4 × 10^{-12}**
L = Cbl	–	74 ± 10	4 ± 1 × 10^{-7}	5 ± 1 × 10^{-15}
L = Cbl*	–	20–60	10^{-5}–10^{-6}	10^{-13}–10^{-14}
TC + L ⇔ TC–L				
L = CBC	1.0 ± 0.1	64 ± 5	4 ± 1 × 10^{-7}	6 ± 1 × 10^{-15}
L = Cbl	–	68 ± 2	3.2 ± 0.6 × 10^{-7}	5 ± 1 × 10^{-15}
L = Cbl*	–	30–100	10^{-7}	10^{-14}–10^{-15}
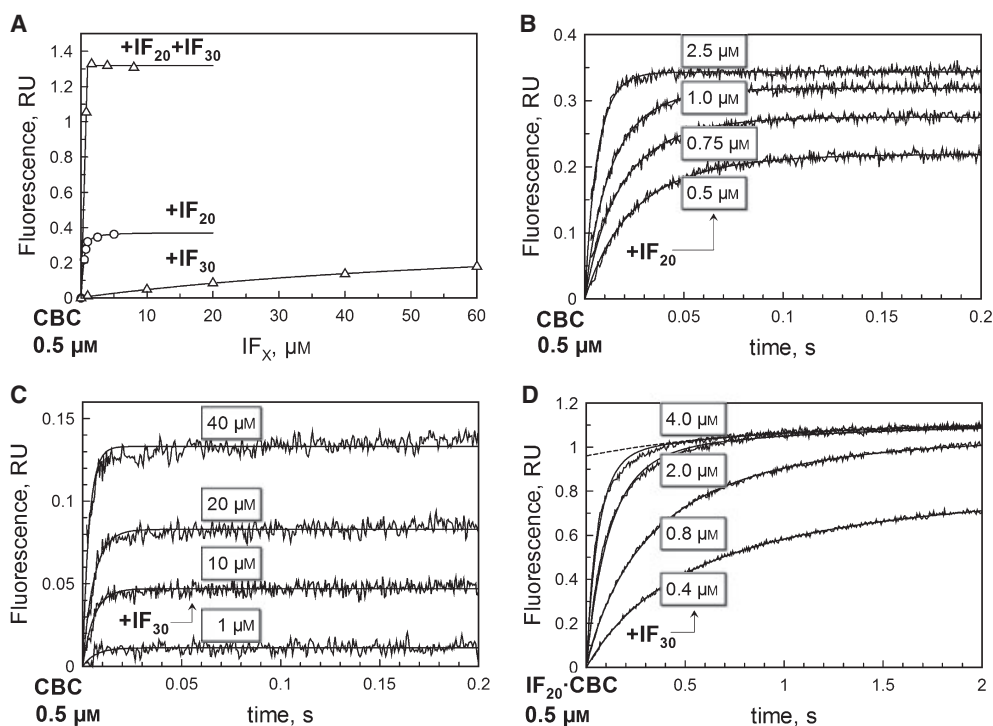
Fig. 3. Binding of CBC to the fragments IF_{20} and IF_{30}. (A) Equilibrium binding of 0.5 μM CBC to IF_{20}, IF_{30} and IF_{20} + IF_{30}. The amplitude of the fluorescent response in equilibrium was measured at 1–5 s from the reaction start. The fluorescence level did not change during this time interval. (B) Time-dependent change in fluorescence induced by binding of [CBC] = 0.5 μM to [IF_{20}] = 0.5, 0.75, 1.0, 2.5 μM. (C) Time-dependent binding of [CBC] = 0.5 μM to [IF_{30}] = 1, 10, 20, 40 μM. (D) Time-dependent binding of [IF_{20}–CBC] = 0.5 μM to [IF_{30}] = 0.4, 0.8, 2, 4 μM. See text and Table 1.

IF_{20} + IF_{30} + CBC at the concentrations used. The curves were fitted by the square-root equation [10] to estimate the maximal amplitude of response ΔF and the equilibrium dissociation constants. The small glyco-peptide IF_{20} had relatively high affinity for the fluorescent ligand with $K_{CBC,20} = 0.13 \pm 0.04$ μM. On the contrary, the binding of CBC to the larger fragment IF_{30} was much weaker, $K_{CBC,30} = 83 \pm 14$ μM. Similar results were found earlier for Cbl as well [10]. The maximal amplitude of fluorescent response for the isolated peptides was relatively low when compared to the three component mixture IF_{30} + IF_{20} + CBC and the full length IF (Fig. 3A and Table 1).

The time course of the binding between CBC and peptides is presented in Fig. 3B,C. The corresponding rate constants k_{+CBC} and k_{-CBC} for IF_{20} and IF_{30} were calculated as described earlier [10], and the results are presented in Table 1. The obtained values were comparable with those known for H_2OCbl [10].

Association of the fragments IF_{20}–CBC + IF_{30}

When the preformed complex IF_{20}–CBC was mixed with the low affinity unit IF_{30} a noticeable increase in

the fluorescence was observed over time (Fig. 3D). It was ascribed to association of two IF fragments into a complex IF_{20}–CBC–IF_{30} as was observed earlier for the true substrate Cbl [9,10]. The main phase [$\Delta F = 2.0$ response units (RU)·μM^{-1}] presumably reflected the bi-molecular reaction IF_{20}–CBC + IF_{30} IF → $_{20}$–CBC–IF_{30} with $k_{F20+30} = 4.2 \pm 0.4$ μM^{-1}·s^{-1}. An additional mono-molecular transition A → B with $k = 1.2 \pm 0.2$ s^{-1} was observed at the end of the reaction. This slow exponential phase accounted for a relatively small increase in the fluorescent signal ($\Delta F = 0.15$ RU·μM^{-1}). Possible explanation of this effect is presented below.

Competitive binding of CBC and Cbl, calculation of k_+

We have tested the application of the fluorescent ana-logue CBC as a tool for investigation of the binding kinetics of nonfluorescent ligands. Cyano-cobalamin (CNCbl) was examined in the present setup. Simul-taneous injection of CBC and Cbl to the specific binding protein (either IF or TC) led to a competitive binding of the two ligands (Fig. 4). The reaction
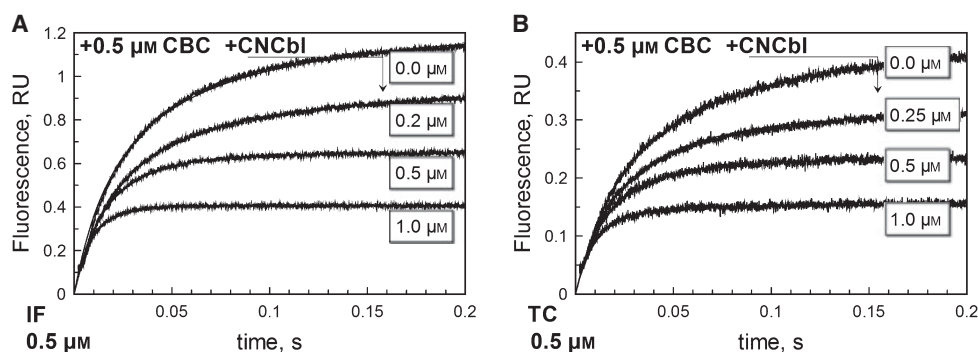
Fig. 4. Competition between CBC and CNCbl for the binding to the transport proteins. (A) Binding of [CBC] = 0.5 μM to [IF] = 0.5 μM in the presence of different Cbl concentrations (0, 0.2, 0.5, 1.0 μM). (B) Binding of [CBC] = 0.5 μM to [TC] = 0.5 μM at different Cbl concentrations (0, 0.25, 0.5, 1.0 μM). See text and Table 1 for details.

obeyed a bidirectional irreversible mechanism, e.g., IF–Cbl ← Cbl + IF + CBC → IF–CBC, at least in the shown time scale. The corresponding rate constants k_{+Cbl} and k_{+CBC} were calculated by computer simulations (see below), and their values appeared to be quite similar, $k_+ = 60–70 \ \mu M^{-1} \cdot s^{-1}$ (Table 1). The obtained results demonstrated good correlation with earlier data for H_2OCbl and CNCbl [14,15].
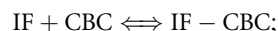
Dissociation of IF–CBC and IF–Cbl in 'chase' experiments

When measuring CBC dissociation, the binding proteins were first loaded with the fluorescent probe and then exposed to a four-fold excess of Cbl. Presence of Cbl caused gradual decrease in the total fluorescence ascribed to dissociation of CBC. Detachment of Cbl was monitored in the opposite manner. The binding protein was initially saturated with Cbl, and then the fluorescent probe was added. The latter displaced Cbl in the binding site, and an increase of fluorescence was registered. Dissociation of the initially bound ligand was expected to be the rate limiting step in all above cases. Control samples (CBC + Cbl and IF–CBC without additives) were also monitored throughout the experiment, see below.

The charts for dissociation of IF–CBC and IF–Cbl versus time are shown in Fig. 5A. Already a rough comparison of the dissociation velocities indicated at least a 10-fold faster liberation of the fluorescent analogue when compared with Cbl. The CBC dissociation spanned at least 90% of the total amplitude, which allows one to describe the reaction as a unidirectional process and fit it by exponential approximation. Surprisingly, the mono-exponential fit was quite inadequate (dotted line, Fig. 5A), and the data were analysed by a double-exponential function instead. Approximately 25% of CBC was liberated with $k_{-1} \approx 2 \times 10^{-4} \ s^{-1}$,

whereas dissociation of the following 65–75% was characterized by $k_{-2} \approx 8 \times 10^{-6} \ s^{-1}$. Possible explanation of the multiphasic kinetics is presented below.

Dissociation of IF–Cbl in the presence of CBC was hardly noticeable (Fig. 5A, bottom curve). An approximate value of k_{-Cbl} was estimated from the initial slope equal to $v_0 = k_{-Cbl} \cdot [IF–Cbl]$ (Fig. 5A, dashed line). We have verified the dissociation process by simulating its behaviour with help of the below scheme:

$$IF + CBC \Longleftrightarrow IF - CBC;$$
$$k_{+CBC} = 70 \ \mu M^{-1} \cdot s^{-1}, k_{-CBC} = 1 \times 10^{-5} s^{-1}$$
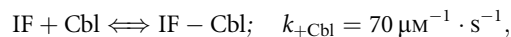
$$IF + Cbl \Longleftrightarrow IF - Cbl; \quad k_{+Cbl} = 70 \ \mu M^{-1} \cdot s^{-1},$$
$$k_{-Cbl} \text{ is the fitting parameter.}$$

The unknown rate constant, obtained from the best fit, corresponded to $k_{-Cbl} = 4 \times 10^{-7} \ s^{-1}$.

Dissociation of TC–ligand complexes

In contrast to IF, dissociation of two TC–ligand complexes occurred equally slowly (Fig. 5B). The corresponding rate constants (Table 1) were calculated from the initial slopes: $v_{0, CBC} = -k_{-CBC} \cdot [TC–CBC]_0$ and $v_{0, Cbl} = k_{-Cbl} \cdot [TC–Cbl]_0$.

Dissociation of the cleaved IF–ligand complexes

The assembled peptide–ligand complexes $IF_{30}–CBC–IF_{20}$ and $IF_{30}–Cbl–IF_{20}$ were exposed to the external substitutes, Cbl or CBC, respectively. This caused dissociation of the original structures and recombination of the peptides with the added ligand. Considering the already known rate constants, the rate-limiting step of the whole process was expected to be detachment of IF_{30} from the assembled complex, e.g., $IF_{30}–CBC–IF_{20} \rightarrow IF_{30} + CBC–IF_{20}$.

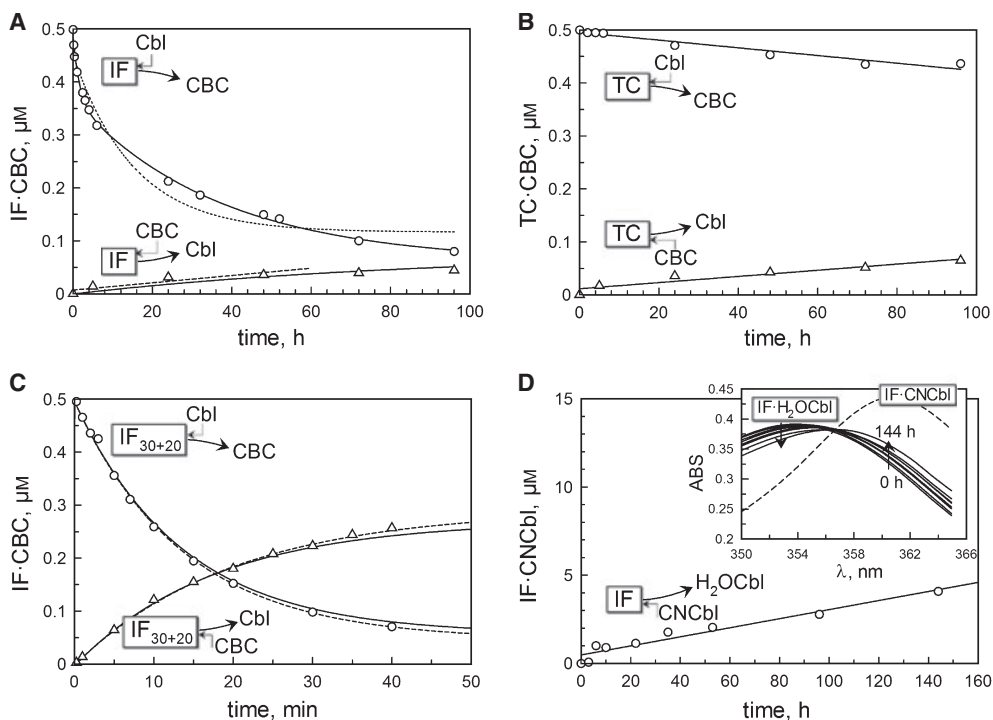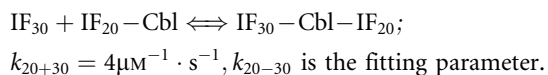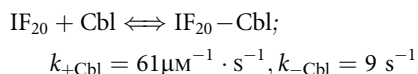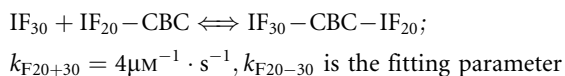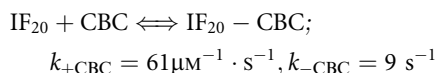**Fig. 5.** Dissociation of the protein-ligand complexes. (A) IF–ligand dissociation followed by fluorescence method: [IF–CBC] = 0.5 μM, [Cbl] = 2 μM (top curve); and [IF–Cbl] = 0.5 μM, [CBC] = 0.55 μM (bottom curve). (B) TC–ligand dissociation followed by fluorescence method: [TC–CBC] = 0.5 μM, [Cbl] = 2 μM (top curve); and [TC–Cbl] = 0.5 μM, [CBC] = 1 μM (bottom curve). (C) Dissociation of IF fragments followed by fluorescence method: IF_{30}–CBC–IF_{20} = (0.6 μM IF_{30} + 0.5 μM CBC + 0.5 μM IF_{20}), [Cbl] = 2 μM (top curve); and IF_{30}–Cbl–IF_{20} = (0.6 μM IF_{30} + 0.5 μM Cbl + 0.5 μM IF_{20}), [CBC] = 1 μM (bottom curve). (D) Dissociation of IF–ligand followed by absorbance method: [IF–H_2OCbl] = 15 μM, [CNCbl] = 50 μM; inset presents transition in the absorbance spectra of the protein-associated ligands IF–H_2OCbl → IF–CNCbl.

As seen from the data in Fig. 5C, stability of both IF_{30}–Cbl–IF_{20} and IF_{30}–CBC–IF_{20} was lower than that of the full length protein (Fig. 5A), and the original structures dissociated in one hour. Rough evaluation revealed a three-fold faster disassembly of IF_{30}–CBC–IF_{20} (curve at the top) when compared with IF_{30}–Cbl–IF_{20} (curve at the bottom). All other interactions seemed to be the same for both ligands, considering the final equilibrium levels at time → ∞ and the concentrations of the reagents used. The whole process was computer simulated according to the below scheme:

$$IF_{20} + CBC \Longleftrightarrow IF_{20} - CBC;$$
$$k_{+CBC} = 61 \mu M^{-1} \cdot s^{-1}, k_{-CBC} = 9 \ s^{-1}$$

$$IF_{30} + IF_{20} - CBC \Longleftrightarrow IF_{30} - CBC - IF_{20};$$
$$k_{F20+30} = 4 \mu M^{-1} \cdot s^{-1}, k_{F20-30} \text{ is the fitting parameter}$$

$$IF_{20} + Cbl \Longleftrightarrow IF_{20} - Cbl;$$
$$k_{+Cbl} = 61 \mu M^{-1} \cdot s^{-1}, k_{-Cbl} = 9 \ s^{-1}$$

$$IF_{30} + IF_{20} - Cbl \Longleftrightarrow IF_{30} - Cbl - IF_{20};$$
$$k_{20+30} = 4 \mu M^{-1} \cdot s^{-1}, k_{20-30} \text{ is the fitting parameter.}$$

Binding of the free ligands to IF_{30} was ignored as insignificant under conditions of the experiment. Optimal values of the fitting parameters k_{F20-30} and k_{20-30} were found for each curve: $1.2 \times 10^{-3} \ s^{-1}$ and $3.6 \times 10^{-4} \ s^{-1}$ (top dashed curve, Fig. 5C); $9.0 \times 10^{-4} \ s^{-1}$ and $5.0 \times 10^{-4} \ s^{-1}$ (bottom dashed curve, Fig. 5C). Then, the obtained parameters were corrected to get the general fit of the whole system with the same set of coefficients. The solid curves in Fig. 5C show the simulations for k_{20-30} values presented in Table 1.

Reliability of CBC-fluorescence method

The data of CBC-based measurements (Table 1) showed a good correlation with the results obtained earlier for Cbls by different methods [10,14,18]. Only the rate constant of IF–Cbl dissociation deviated from our previous data and pointed to better retention of the ligand by the current protein preparation (Table 1). The difference could be caused by either changed renaturing procedure for IF or inaccuracy of one of the kinetic methods. In order to verify the current data of
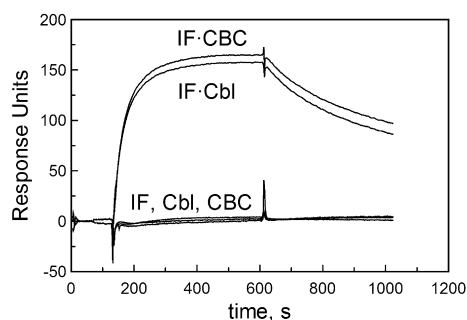
Fig. 6. Interaction of IF with the receptor-coated BIACore chip in the presence or absence of the ligand. At time 120 s IF was added to the receptor-coated chip either alone (bottom curve) or in complex with Cbl or CBC (top curves). Washing out procedure was started at $t = 600$ s. Free ligands (Cbl, CBC) did not affect the baseline (bottom curves).

fluorescent measurements we repeated the dissociation experiment with IF according to the previously described method [10], where change in the absorbance spectrum of IF–Cbl was measured upon displacement of H_2OCbl by CNCbl, Fig. 5D. The estimated value of $k_{-H_2OCbl} = 5 \times 10^{-7}$ s^{-1} corroborated higher stability of IF–Cbl from the current protein preparation.

Binding of IF–CBC and IF–Cbl to the specific receptor

Binding of two protein–ligand complexes IF–CBC and IF–Cbl to the receptor cubilin was tested by surface plasmon resonance. Identical pattern of records (Fig. 6) implied that both complexes were recognized by the receptor equally well. The experiment suggests that the tertiary structure of the receptor recognition site in IF–CBC is indistinguishable from that of IF–Cbl.

Discussion

In the present article we demonstrate that the fluorescent Cbl analogue CBC (Fig. 1A) binds to the transporting proteins TC and IF. Interaction of CBC with the Cbl specific proteins was accompanied by significant change in its fluorescence (Fig. 1B). Therefore, the binding-dissociation reactions could be monitored directly in time making this fluorescent conjugate particularly suitable for refined analysis of the Cbl binding kinetics.

Interaction between CBC and TC was not affected by presence of the 5'O-ribosyl conjugated fluorophore, as was expected from the crystallographic data for TC–Cbl complex [16], and the binding-dissociation curves of CBC and Cbl were identical (Figs 2B,4B

and 5B, Table 1). Using a new and more sensitive approach we confirm correctness of the lowest equilibrium dissociation constants for TC–Cbl and TC–CBC complexes $(K_d = 5 \times 10^{-15}$ M$^{-1})$. Impressive dissociation stability of TC–CBC implies its essential resemblance to TC–Cbl, and therefore, suggests normal transportation of the fluorescent probe in the organism, especially taking into account moderate variation of the receptor affinity for apo-/holo-TC [21,22].

Attachment of CBC to the most Cbl-specific protein IF was fast and matched the binding velocity of Cbl, $k_{+CBC} \approx k_{+Cbl} \approx 70 \times 10^6$ M^{-1}·s^{-1} (Table 1). Detachment of CBC from IF was, however, accelerated by a factor of 20 (Fig. 5A, main phase). Regardless the latter fact, retention of CBC by IF was still formidable with $K_d = 120$ fM for 65–75% of the protein. This seems to be quite enough to bind the ligand under physiological conditions (IF ≈ 50 nM).

Another interesting observation concerns biphasic dissociation of IF–CBC with $k_{-1CBC} = 2 \times 10^{-4}$ s^{-1} for the fast phase (25%) and $k_{-2CBC} = 8 \times 10^{-5}$ s^{-1} for the slow one (65–75%), (Fig. 5A, upper curve). We do not think that the effect is caused by the original heterogeneity of IF preparation because the protein was homogeneous in all other respects. An alternative explanation seems to be more probable. Thus, distorted shape of the analogue causes partial corruption of its bonds with IF. As a consequence, the ligand and the protein form several complexes with different dissociation stability being in equilibrium, e.g., (IF–CBC)$_1$ $\Leftrightarrow$ (IF–CBC)$_2$. If transition between these conformations is sufficiently slow, dissociation of the ligand would be described by two to three rate coefficients (which was, indeed, observed). No such effect was found for dissociation of TC–CBC which was in all respects indistinguishable from that of TC–Cbl (Fig. 5B). We can therefore surmise that the sufficiently wide opening at 5' OH-ribosyl group found in TC–Cbl complex [16] might be quite narrow in IF–Cbl. Consequently, the bonding of CBC at its conjugated 5' O-ribosyl group is partially unaccomplished in IF. Presence of a slow equilibrium at this site (e.g., bound $\leftrightarrow$ unbound) may account for the discussed biphasic dissociation of IF–CBC. The general structure of the obtained IF–CBC complex was, however, close to IF–Cbl, because both of them bound to the specific receptor cubilin in a uniform manner (Fig. 6).

It is known that IF is the most Cbl-specific binder among three transporting proteins [5,7]. This feature makes the mechanism of interaction between IF and the ligand especially interesting as a kinetic example of the utmost substrate selectivity. We have earlier suggested a two domain organization of IF, where the

distant units IF_{30} and IF_{20} are assembled by the substrate into a firm complex [9,10]. This architecture of the Cbl-transporting proteins was directly demonstrated by crystallographic studies of TC [16], another member of this family. Highly sensitive fluorescent analogue provided an opportunity to investigate individual contributions of different domains to the process of substrate recognition, using the fragments IF_{30} and IF_{20} as a model.

Binding of CBC to the isolated fragments IF_{20} and IF_{30} closely resembled that for Cbl (Fig. 5C, Table 1). In other words, two domains were not very specific if taken separately, at least in the example shown. Lacking specificity for ligands seems to be caused by insufficient contact area in each domain. Indeed, the maximal fluorescent signal in the two-component mixtures IF_{20} + CBC and IF_{30} + CBC (30% and 30%) was lower than that in the complete three-component mixture IF_{20} + CBC + IF_{30} (100%). This observation points to a reduced number of potential protein–ligand bonds when the two domains are taken apart. On the other hand, simultaneous interaction of the two fragments/domains with the sandwiched ligand had a cooperative character. It leads to higher fluorescent response and better fixation of CBC. Final stabilization of IF_{30}–CBC–IF_{20} can occur after series of transitions at the domain–domain interface, which may be the reason for the slow exponential phase during interaction of IF_{20}–CBC with IF_{30} (Fig. 3D).

The discussed interdomain adjustments are expected to be dependent on the geometry of ligands placed in-between. Presence of a substrate with inappropriate shape would disturb IF_{30}–IF_{20} interface and decrease stability of the final protein–ligand complex, possibly creating several 'erroneous' or alternative conformations. The weaker ligand retention and biphasic dissociation kinetics of IF–CBC (Fig. 5A) are in agreement with the presented speculations. The peptide link, which connects the two domains in the full length protein, is not just a spectator of protein–ligand interactions. Thus, it adds to both ligand affinity and specificity of IF. This statement is based on the following observations: (a) the uncleaved IF retained Cbl/CBC better than the separated fragments 'glued' by the ligand (Fig. 5A and C, respectively); (b) discrimination between CBC and Cbl was better expressed for the full length protein (20-fold difference) than for the peptides (three-fold difference). It is possible that the 'right' or 'wrong' positioning of the domains by the link prior to the substrate binding partially accounts for different specificity of IF, TC and HC for Cbl. The probable scheme of interaction between IF, the ligand and the receptor is presented in
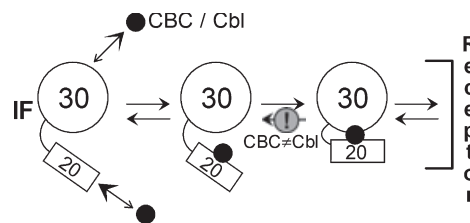

Fig. 7. Schematic presentation of IF interaction with the ligands and the receptor. Both CBC and Cbl (filled circles) bind preferentially to IF_{20} domain, thus inducing assembly of IF_{20}–S and IF_{30} units into a composite structure recognized by the receptor. The ligand binding step, which seems to be responsible for reduced affinity for the analogue, is indicated with '!' sign.

Fig. 7. The step(s) responsible for discrimination between CBC and Cbl is specified.

It is generally accepted that IF serves as a reliable shield, protecting organisms against uptake of corrinoids with deviating structure. Yet, calculations show that IF would be partially saturated under physiological concentrations of this protein ($\approx$ 50 nM) even if the affinity for a ligand is decreased by a factor of 10^6 (e.g., to K_d = 1–10 nM). Additional observation indicates that the reduced affinity for the analogue CBC had no effect on the recognition of IF–CBC complex by the specific receptor cubilin immobilized on the detecting chip (Fig. 6). All the above facts mean that the intestinal uptake of analogues can be quite feasible. In this regard we plan to examine a group of analogues concerning details of their binding to the specific proteins and receptors.

In conclusion, the binding of a fluorescent Cbl analogue (CBC) to two Cbl-transporting proteins TC and IF was found to be 'normal' and 'close to normal', respectively. Applicability of CBC as a tool for analysis of the binding kinetics was established and allowed to make several inferences concerning the protein–ligand and protein–receptor interactions. Furthermore, our results provide strong arguments that the transportation routes of CBC and Cbl would be identical in the human body. CBC appears to be useful for tracing accumulation of vitamin B_{12} in cancer cells and other tissues.

Experimental procedures

Materials

All standard chemicals were purchased from Merck (Whitehouse Station, NJ, USA), Roche Molecular Biochemicals (Mannheim, Germany), Sigma-Aldrich (Cambridge, MA, USA). $H_2OCbl/CNCbl$ and ^{57}Co-labeled Cbl were obtained from Sigma-Aldrich and ICN Pharmaceutical Ltd (Costa Mesa, CA, USA), respectively.

Methods

Expression and purification of human recombinant IF and TC

The recombinant Cbl binding proteins and their fragments were isolated from plants and yeast as described earlier [9,17]. Preparation of the unsaturated apo-form of IF was although modified. Thus, the Cbl-saturated holo-IF (1 mg·mL^{-1}) was dialysed against 20 volumes of 8 M urea (30 °C) instead of 5 M GdnHCl. The incubation was continued for 4–6 days with three changes of the urea solution. Renaturation was achieved by 1 : 10 dilution with 0.2 M phosphate buffer pH 7.5 at 20 °C. The protein was afterwards concentrated 50 : 1 by ultrafiltration and dialysed against excess of 0.2 M phosphate buffer pH 7.5.

Synthesis of the fluorescent Cbl analogue CBC-244

Activation of the 5′ hydroxyl group in the α-ribofuranoside moiety of CNCbl was performed with help of 1,1′-dicarbonyl-di-(1,2,4-triazole) as described elsewhere [19,20], whereupon 4,7,10-trioxa-1,13-tridecanediamine was conjugated as a spacer [19,20]. Amino group of the spacer was used for the attachment of the fluorophore, 5/6-carboxyrhodamine 6G, succinimidyl ester (5/6 mixed isomers) from Molecular Probes (Eugene, OR, USA), according to recommendations of the manufacturer. The product was a mixture of 5′ and 6′ forms in the ratio 44 : 53. The above isomers were separated by reverse phase HPLC on C-18 column.

Measurement of fluorescence spectra

Excitation spectra of 5′ C-CBC-244 were recorded in the range 400–550 nm (excitation bandpass 3 nm), using emission wavelength 600 nm (bandpass 5 nm). Emission spectra were recorded in the range 500–600 nm (bandpass 5 nm), excitation wavelength 480 nm (bandpass 3 nm).

Measurement of the binding kinetics with fluorescent probe CBC

Increase in fluorescence upon binding of CBC to the Cbl specific proteins was recorded on DX.17 MV stopped-flow spectrofluorometer (Applied Photophysics, Leatherhead, UK), using excitation wavelength 525 nm (bandpass 7 nm) with 550 nm cut-off filter on the emission side. The binding was carried out in 0.2 M phosphate buffer pH 7.5, 20 °C, at 0.5 μM CBC and varying concentrations of the binding protein or peptide (0.5–2.5 μM). All experiments were performed in triplicate, and the average records are presented.

Experiments on competitive binding of CBC and Cbl to the specific proteins (IF or TC) were conducted as described above. Final concentrations of the reagents in the cuvette were 0.5 μM binding protein, 0.5 μM CBC, 0.25–1 μM Cbl.

Measurement of the dissociation kinetics with the fluorescent probe CBC

A ligand exchange method was used in the below 'chase' experiments, e.g., IF–CBC + Cbl → IF–Cbl + CBC. Changes of the emission spectra were recorded over time in the mixtures protein–CBC (0.5 μM) + Cbl (2 μM) or protein–Cbl (0.5 μM) + CBC (0.55–1 μM) when measuring dissociation of CBC or Cbl, respectively. Two control samples for each binding protein contained (i) protein–CBC (0.5 μM) and (ii) CBC (0.5 μM) + Cbl (2 μM) or Cbl (0.5 μM) + CBC (0.55–1 μM). The concentration of protein–CBC complex (e.g., for IF) at time t was calculated according to the equation:

$$\mathrm{IF} \cdot \mathrm{CBC}_t = \frac{F_{\mathrm{sample}} - F_{\mathrm{min}}}{q \cdot F_{\mathrm{max}} - F_{\mathrm{min}}} \cdot IF_0$$

where F_{sample} is fluorescence of the experimental sample (e.g., IF–CBC + Cbl or IF–Cbl + CBC) at time t; q is a quenching coefficient determined separately for the corresponding mixture (example in Fig. 2C); parameters F_{max} and F_{min} correspond to the control probes (e.g., IF–CBC and CBC + Cbl) and indicate the maximal and minimal possible fluorescence for the experimental sample; IF_0 corresponds to the total concentration of the binding sites.

Measurement of the dissociation kinetics by absorbance method

This procedure was described earlier [10]. Briefly, the mixture of IF–H$_2$OCbl (15 μM) and CNCbl (50 μM) in P$_i$ buffer, pH 7.5, 20 °C was incubated over time. Free ligands were adsorbed on charcoal, and the absorbance spectra were recorded. Concentration of appearing IF–CNCbl was calculated by comparison with the standards IF–H$_2$OCbl and IF–CNCbl according to the equation:

$$\mathrm{IF} \cdot \mathrm{CNCbl}_t = \frac{(\Delta A_{352} + \Delta A_{361})}{(\Delta A_{352}^{\mathrm{max}} + \Delta A_{361}^{\mathrm{max}})} \cdot IF_0$$

where, e.g., ΔA_{352} corresponds to change of absorbance at wavelength 352 nm in the reaction sample after incubation time t; $\Delta A_{352}^{\mathrm{max}} = |A_{\mathrm{CNCbl}} - A_{\mathrm{H_2OCbl}}|$ stands for maximal possible change in the amplitude at wavelength, e.g. 352 nm; IF_0 represents total concentration of the binding sites.

Binding of IF to the receptor

IF, with or without ligands, interacted with the specific receptor cubilin immobilized on the surface of the detecting chip in BIACore 2000 instrument (Biacore International AB, Uppsala, Sweden) [24].

Data processing

The data for irreversible and reversible bimolecular reactions $E + S \rightarrow ES$ and $E + S \Leftrightarrow ES$ (Figs 3 and 4) were subjected to nonlinear regression analysis using the appropriate equations [10]. The rate constants k_{+S} and k_{-S} were calculated by a fitting program KYPLOT 4 (Kyence Lab Inc., Tokyo, Japan). Complex reactions without algebraic solution were simulated and fitted using program GEPASI 3.2 (http://www.gepasi.org) [23] supplied by kinetic schemes presented in the main text.

Acknowledgements

References

1 Banerjee R & Ragsdale RW (2003) The many faces of vitamin B12: catalysis by cobalamin-dependent enzymes. *Annu Rev Biochem* **72**, 209–247.

2 Russell-Jones GJ (1998) Use of vitamin B12 conjugates to deliver protein drugs by the oral route. *Crit Rev Ther Drug Carrier Syst* **15**, 557–586.

3 Collins DA, Hogenkamp HP, O'Connor MK, Naylor S, Benson LM, Hardyman TJ & Thorson LM (2000) Biodistribution of radiolabeled adenosylcobalamin in patients diagnosed with various malignancies. *Mayo Clin Proc* **75**, 568–580.

4 Bagnato JD, Eilers AL, Horton RA & Grissom CB (2004) Synthesis and characterization of a cobalamin-colchicine conjugate as a novel tumor-targeted cyto-toxin. *J Org Chem* **69**, 8987–8996.

5 Allen RH (1975) Human vitamin B12 transport proteins. *Prog Hematol* **9**, 57–84.

6 Grasbeck R (1984) Biochemistry and clinical chemistry of vitamin B12 transport and the related diseases. *Clin Biochem* **17**, 99–107.

7 Nexø E (1998) Cobalamin binding proteins. In *Vitamin B12 and B12-Proteins* (Kräutler B, Arigoni D & Golding T, eds), pp. 461–475. Wiley-VCH, Weinheim, Germany.

8 Moestrup SK & Verroust PJ (2001) Megalin- and cubilin-mediated endocytosis of protein-bound vitamins, lipids, and hormones in polarized epithelia. *Annu Rev Nutr* **21**, 407–428.

9 Fedosov SN, Fedosova NU, Berglund L, Moestrup SK, Nexø E & Petersen TE (2004) Assembly of the intrinsic factor domains and oligomerization of the protein in the presence of cobalamin. *Biochemistry* **43**, 15095–15102.

10 Fedosov SN, Fedosova NU, Berglund L, Moestrup SK, Nexø E & Petersen TE (2005) Composite organization of the cobalamin binding and cubilin recognition sites of intrinsic factor. *Biochemistry* **44**, 3604–3614.

11 Hippe E, Haber E & Olesen H (1971) Nature of vitamin B12 binding. II. Steric orientation of vitamin B12 on binding and number of combining sites of human intrinsic factor and the transcobalamins. *Biochim Biophys Acta* **243**, 75–82.

12 Marchaj A, Jacobsen DW, Savon SR & Brown KL (1995) Kinetics and termodynamics of the interaction of cyanocobalamin (vitamin B12) with haptocorrin: measurement of the highest protein-ligand binding constant yet reported. *J Am Chem Soc* **117**, 11640–11646.

13 Brada N, Gordon MM, Wen J & Alpers DH (2001) Transfer of cobalamin from intrinsic factor to transcobalamin II. *J Nutr Biochem* **12**, 200–206.

14 Fedosov SN, Berglund L, Fedosova NU, Nexo E & Petersen TE (2002) Comparative analysis of cobalamin binding kinetics and ligand protection for intrinsic factor, transcobalamin, and haptocorrin. *J Biol Chem* **277**, 9989–9996.

15 Cannon MJ, Myszka DG, Bagnato JD, Alpers DH, West FG & Grissom CB (2002) Equilibrium and kinetic analyses of the interactions between vitamin B12 binding proteins and cobalamins by surface plasmon resonance. *Anal Biochem* **305**, 1–9.

16 Wuerges J, Garau G, Geremia S, Fedosov SN, Petersen TE & Randaccio L (2006) Structural basis for mammalian vitamin B12 transport by transcobalamin. *Proc Natl Acad Sci USA* **103**, 4386–4391.

17 Fedosov SN, Laursen NB, Nexø E, Moestrup SK, Petersen TE, Jensen EØ & Berglund L (2003) Human intrinsic factor expressed in the plant *Arabidopsis thaliana*. *Eur J Biochem* **270**, 3362–3367.

18 Fedosov SN, Fedosova NU, Nexø E & Petersen TE (2000) Conformational changes of transcobalamin induced by aquocobalamin binding. Mechanism of substitution of the cobalt-coordinated group in the bound ligand. *J Biol Chem* **275**, 11791–11798.

19 McEwan JF, Veitch HS & Russel-Jones GJ (1999) Synthesis and biological activity of 5′-ribose-carbamate derivatives of vitamin B12. *Bioconjug Chem* **10**, 1131–1136.

20 Horton RA, Bagnato JD & Grissom CB (2003) Structural determination of 5′-OH á-ribofuranoside modified cobalamins via ^{13}C and DEPT NMR. *J Org Chem* **68**, 7108–7111.

21 Seligman PA & Allen RH (1978) Characterization of the receptor for transcobalamin II isolated from human placenta. *J Biol Chem* **253**, 1766–1772.

22 Quadros EV, Nakayama Y & Sequeira JM (2005) The binding properties of the human receptor for the cellular uptake of vitamin B12. *Biochem Biophys Res Commun* **327**, 1006–1010.

23 Mendes P (1997) Biochemistry by numbers: simulation of biochemical pathways with Gepasi 3. *Trends Biochem Sci* **22**, 361–363.

24 Birn H, Verroust PJ, Nexø E, Hager H, Jacobsen C, Christensen EI & Moestrup SK (1997) Characterization of an epithelial ~460 kDa protein that facilitates endocytosis of intrinsic factor-vitamin B_{12} and binds receptor associated protein. *J Biol Chem* **272**, 26497–26504.